A Novel Phasor Power Oscillation Damper With Adaptive Phase Compensation, Achieved Using Multiple Model Adaptive Estimation

Haugdal, Hallvar; Uhlen, Kjetil; Jóhannsson, Hjörtur

Published in:
IEEE Transactions on Power Systems

Link to article, DOI:
10.1109/TPWRS.2022.3202239

Publication date:
2023

Document Version
Peer reviewed version

A Novel Phasor Power Oscillation Damper with Adaptive Phase Compensation, achieved using Multiple Model Adaptive Estimation

Hallvar Haugdal, *Student Member, IEEE,* Kjetil Uhlen, *Member, IEEE,* and Hjörtur Jóhannsson, *Member, IEEE,*

***Abstract*—In this paper, an adaptive version of the well known Phasor Power Oscillation Damper is presented. The proposed controller is adaptive in the sense that the phase compensation between the measured input and the applied control action is adjusted online during changing operating conditions. This is achieved through Multiple Model Adaptive Estimation, where a bank of Kalman filter estimators are run in parallel. A system model is inferred by assessing the performance of the individual filters, and used to update the tuning of the controller online.**

The proposed adaptive phase compensation scheme is compared with a similar scheme found in the literature, and is found to exhibit superior performance under the tested conditions. Simulation results from the Single-Machine Infinite Bus system, Kundur's Two-Area System and the IEEE 39-Bus System demonstrate that the proposed controller is able to adjust the phase compensation in response to severe non-linear events, and to eliminate phase lag due to communication latency.

***Index Terms*—Phasor estimation, Kalman filtering, thyristor controlled series capacitor (TCSC), power oscillation damper (POD), multiple model adaptive estimation (MMAE), adaptive control.**

I. Introduction

PROBLEMATIC electromechanical oscillations appear regularly in power systems around the world. Global trends like increasing penetration of renewable energy sources, increasing electricity demand and increasing import and export of energy between countries cause larger and less predictable fluctuations in both generation and demand. This makes it more difficult to design and tune control systems responsible for stabilizing oscillations, since stability must be ensured for a wider range of expected operating conditions. Adding that the frequency of extreme weather events is increasing due to climate change, the system must also be expected to end up in unscheduled operating points more often. Under such circumstances, for instance unusually high or low loading in combination with loss of crucial equipment or disconnection of important lines, conventional stabilizing control systems like Power System Stabilizers (PSS) are not always effective. Such circumstances resulted in unstable oscillations in the often mentioned 1996 WSCC System Outage [1], and also in more recent events in Europe, e.g. [2], [3].

H. Haugdal and K. Uhlen are with the Department of Electrical Power Engineering, Norwegian University of Science and Technology, Trondheim, Norway (e-mail: hallvar.haugdal@ntnu.no, kjetil.uhlen@ntnu.no).

H. Jóhannsson is with the Department of Electrical Engineering, Technical University of Denmark, Kgs. Lyngby 2800, Denmark (e-mail: hjjo@elektro.dtu.dk).

As a means of providing damping in situations where conventional PSS are not effective, the Phasor Power Oscillation Damper (P-POD) was introduced in [4]. Characteristic to the operation of the P-POD is that a phasor is estimated from the measured signal, representing the instantaneous phase and amplitude of power oscillations of a given frequency, and the control signal is generated by applying an appropriate phase shift to the estimated phasor. In [4], the phasor is estimated from the measured power flow on an inter-tie, and the control signal modulates the reactance setpoint of a Thyristor Controlled Series Capacitor (TCSC) installed on the line. A phase shift of 90° is used between the measured oscillations and the applied control signal.

An advantage of the P-POD introduced in [4] is that the tuning procedure is intuitive and simple compared to many other solutions, which require, e.g., tuning of cascaded filters in order to achieve the desired phase compensation. In many cases, there is one problematic, dominant inter-area mode for which sufficient damping must be ensured. Applying the P-POD, the frequency of the targeted low-damped mode, the desired phase compensation and the gain are specified directly as parameters of the controller. Further, using the mentioned phase compensation of 90° proposed in [4] allows the controller to be applied also without searching for a suitable phase compensation, requiring only the mode frequency and the gain to be specified. It should be mentioned also that extensions of the P-POD estimation algorithm to accommodate multiple low damped modes are described in the literature, e.g. [5].

In [6], the authors elaborate on the limitations and challenges of the original P-POD. Specifically, it is shown that a phase compensation of 90° is not necessarily optimal for the configuration in [4], and that the ideal compensation also varies with the operating conditions. It is further concluded that "an adaptive phase shift scheduling mechanism...needs to be devised".

Applying the P-POD in a wide-area framework is addressed in [7] and [8], where remote PMU measurements serve as the measurement to the controller. This allows the measurement with the highest observability of the targeted mode to be selected as the input to the controller, potentially facilitating a more effective damping control signal, but also introduces two challenges: First, the communication latency must be compensated; Second, a suitable phase compensation must be determined. Both issues are addressed in [7] and [8], where the main focus is on latency compensation. For the phase compensation, an adaptive scheme is proposed in [7]. Specif-

ically, the phase compensation is controlled by a Proportional Integral (PI) controller driving the magnitude of oscillations towards zero. One apparent disadvantage of this scheme is that if the P-POD is not able to eliminate oscillations completely, then the integrator will continue increasing monotonically, eventually causing the controller to amplify oscillations rather than mitigate oscillations for a period of time. Thus, the PI controlled phase compensation has an inherent problem with robustness. The same adaptive phase compensation scheme is adopted in the Enhanced APPOD (EAPPOD) proposed in [8], where the damping control action is applied through a Doubly Fed Induction Machine (DFIG) in a wind power plant.

In this paper, we contribute with an alternative way of controlling the phase compensation of the P-POD, which does not exhibit the outlined weakness of the PI control-based adaptive phase compensation scheme, and thus is more robust. Adjusting the phase compensation continually results in a controller which is capable of adjusting to changing operating conditions. This facilitates the application of the P-POD in a wide-area framework, but is also beneficial in a local configuration (i.e., a P-POD operating with local measurements).

Other previously described adaptive functionality for the P-POD in the literature includes, among other, frequency correction [4] and increased phasor estimation accuracy during transient conditions using a recursive least squares algorithm with variable forgetting factor [9]. To the knowledge of the authors, no other *adaptive phase compensation* schemes for the P-POD are described in the literature (other than the PI-controlled phase compensation mentioned above). Thus, this is what we seek to contribute with in this paper.

In most variants of the P-POD described in the literature, the phasor estimation is carried out using Low Pass Filters or Recursive Least Squares, where the only source of information for the estimator is the chosen output measurement. In recent research, the potential benefit of including the control signal applied by the P-POD in the estimation is explored, since this information is obviously always available. In [10], this is achieved by introducing a predictor-corrector estimator in the form of a Kalman Filter; specifically, the amplitude and phase of oscillations at the next time step are predicted based on the control signal that the P-POD applies at the current step, and the measurement is used to correct the estimate. The prediction step requires a simple system model which is determined by the transfer function residue of the targeted low damped mode, where the transfer function is from the applied control signal to the output measurement.

In this paper, we make use of the predictor-corrector estimator introduced in [10] to develop the P-POD into an adaptive controller, which is adaptive in the sense that the phase compensation is adjusted automatically during changing operating conditions. This is achieved by introducing a Multiple Model Adaptive Estimation scheme: A number of Kalman filters are running in parallel, each making predictions based on a specific, assigned transfer function residue. By assessing the accuracy of the individual estimators, the actual value of the residue can be inferred. The phase compensation is adjusted according to the residue estimate, resulting in a P-POD with adaptive phase compensation.

During the last decades, many innovative approaches to adaptive power oscillation damping have been proposed in the literature. One approach is to use system identification techniques for estimating a system model from PMU measurements, which can further be used for continuously updating the tuning of stabilizing controls. In [11], a dynamic system matrix is estimated from PMU measurements, which is used to tune the feedback gain matrix in a linear state feedback control scheme. A disadvantage of such approaches is that relatively long time windows are required for the estimation to produce reliable models, i.e. on the scale of minutes. In emergency situations, when the operating point of the system changes rapidly, there might not be time for system identification and re-tuning of controllers before the situation further deteriorates.

In [12], a Multiple Model Adaptive Control scheme is described, which is based on tuning a bank of controllers to a bank of corresponding models describing expected operating conditions of the system. This allows swift adaptation of stabilizing controls in response to a transition from a stable to an unstable operating point. However, the performance of this scheme requires that at least one of the models in the bank accurately resembles the system at its current operating point. In [13], a model-free approach to power oscillation damping is described, where analytical expressions derived for a simplified model are used to tune the controller parameters when standing oscillations occur. However, this scheme might not be effective if the simplified models does not accurately resemble the actual system.

Compared to the above outlined approaches, the adaptive P-POD proposed in this paper has the advantage that it requires very little knowledge about the system to be applied, and does not require identifying a system model. The internal parameters of the controller are updated in a recursive manner, allowing swift adaptation to changing operating conditions. At the current stage of development, it should be emphasized that the magnitude of the mentioned transfer function residue is required to be known in order to apply the controller, but it is expected that only minor modifications are required to eliminate this requirement. This is described in closer detail in Section V.

The proposed adaptive P-POD is first tested on the Single-Machine Infinite Bus system, where we demonstrate the concept and investigate the expected gain in robustness and performance compared to the PI controlled phase compensation scheme used in [7] and [8]. Further, the controller is tested on Kundur's Two-Area System, demonstrating the performance during a severe non-linear event. Finally, results from the IEEE 39-Bus System shows that the controller is capable of eliminating phase lag introduced by communication latency.

The relevant background is described in Section II, the proposed MMAE scheme is developed in Section III, results are given in Section IV, before discussion and conclusions in Sections V and VI, respectively.

II. Background

At the core of the original P-POD [4] is an estimator that decomposes the measured signal into an average component $\bar{S}$ and an oscillatory component, where the latter is represented by a phasor $\vec{S}$:

$$S(t) = \bar{S} + \mathrm{Re}\{\vec{S}e^{j\omega t}\} \tag{1}$$

Here, ω is the assumed frequency (in rad/s) of the targeted oscillatory mode. From the phasor estimate, the control signal is generated by applying a suitable phase shift β and amplification K, and transforming to time domain:

$$u(t) = \mathrm{Re}\left\{Ke^{j\beta}\left(\vec{S}e^{j\omega t}\right)\right\} \tag{2}$$

Assuming a sufficiently accurate power system model is available, a suitable phase shift can be determined from modal analysis. The linearized system on state space form is given as follows [14]:

$$\Delta\dot{\mathbf{x}} = \mathbf{A}\Delta\mathbf{x} + \mathbf{b}\Delta u \tag{3}$$

$$\Delta y = \mathbf{c}\Delta\mathbf{x} \tag{4}$$

Performing an eigendecomposition gives the decoupled system:

$$\dot{\mathbf{z}} = \mathbf{\Lambda}\mathbf{z} + \mathbf{\Psi}\mathbf{b}\Delta u \tag{5}$$

where $\mathbf{\Lambda}$ contains the system eigenvalues on the diagonal, i.e. $\mathbf{\Lambda} = \mathrm{diag}(\lambda_1, \lambda_2 \dots \lambda_n)$. Assuming $\lambda_m = \alpha_m + j\omega_m$ is the eigenvalue corresponding to the low damped mode, and $\boldsymbol{\psi}_m$ and $\boldsymbol{\phi}_m$ are the corresponding left and right eigenvectors, the transfer function residue of the mode is given by

$$r = \mathbf{c}\boldsymbol{\phi}_m\boldsymbol{\psi}_m\mathbf{b} \tag{6}$$

where the transfer function is, again, from the applied control signal to the output measurement. From this residue, the ideal phase compensation can be determined [15]:

$$\beta = 180^\circ - \arg\{r\} \tag{7}$$

This phase compensation can be used directly in (2).

A. Predictor-Corrector Phasor Estimation Scheme

Using a predictor-corrector estimator in the form of a Kalman filter in a P-POD is described in [10]. The phasor at the next step is predicted based on the control signal applied at the current step, and the predicted value is corrected with the measurement. In this section, the resulting expressions from the derivations in [10] are reproduced.

Using a Kalman Filter for a single-input single-output system requires a model on the following form [16]:

$$\mathbf{X}_{k+1} = \mathbf{F}_k\mathbf{X}_k + \mathbf{G}_k u_k + \mathbf{w}_k \tag{8}$$

$$Y_k = \mathbf{H}_k\mathbf{X}_k + v_k \tag{9}$$

Here, $\mathbf{X}_k$ is the Kalman filter states, $\mathbf{F}_k$ is the State Transition Matrix, $\mathbf{G}_k$ is the Control-Input Model, Y_k is the Measurement, $\mathbf{H}_k$ is the Observation Model, $\mathbf{w}_k$ is the Process noise (with covariance matrix $\mathbf{Q}$), v_k is the Measurement noise (with variance R), and k is the time step index.

The states of the filter are chosen as $\mathbf{X}_k = \begin{bmatrix}\bar{S}_k & D_k & Q_k\end{bmatrix}^\intercal$, where $\bar{S}$ is the signal average and D_k and Q_k are the real and imaginary components of the phasor (i.e. $\vec{S} = D_k + jQ_k$). The Kalman Filter measurement is the same as the P-POD measurement, i.e. $Y_k = S_k$. As given in [10], the measurement relates to the states as follows:

$$S_k = \underbrace{\begin{bmatrix}1 & \cos\omega t - \sin\omega t\end{bmatrix}}_{\mathbf{H}_k}\begin{bmatrix}\bar{S}_k \\ D_k \\ Q_k\end{bmatrix} \tag{10}$$

This equation is equivalent to (1), and determines the observation model $\mathbf{H}_k$ of the Kalman filter.

Developing the prediction step (also described in [10]) is achieved by introducing the solution to the State Space formulation. The resulting State Transition Matrix $\mathbf{F}_k$ and the Control-Input Model $\mathbf{G}_k$ are as follows:

$$\begin{bmatrix}\bar{S}_{k+1} \\ D_{k+1} \\ Q_{k+1}\end{bmatrix} = \underbrace{\begin{bmatrix}1 & & \\ & 1 & \\ & & 1\end{bmatrix}}_{\mathbf{F}_k}\begin{bmatrix}\bar{S}_k \\ D_k \\ Q_k\end{bmatrix} + \underbrace{\begin{bmatrix}0 \\ Ug(t) + Vh(t) \\ -Uh(t) + Vg(t)\end{bmatrix}}_{\mathbf{G}_k} u_k \tag{11}$$

The coefficients U and V are determined from the transfer function residue of the low damped mode (with index m), where the transfer function is from the applied control signal to the output measurement:

$$r = \mathbf{c}\boldsymbol{\phi}_m\boldsymbol{\psi}_m\mathbf{b} = U + jV \tag{12}$$

Further, the two time-dependent functions $g(t)$ and $h(t)$ are given by

$$g(t) = \frac{2}{\omega}\Big[-\sin(\omega t) + \sin(\omega(t+\Delta t))\Big] \tag{13}$$

$$h(t) = \frac{2}{\omega}\Big[\cos(\omega t) - \cos(\omega(t+\Delta t))\Big] \tag{14}$$

Regarding tuning of the Kalman filter in terms of covariance matrices, the following expressions are proposed in [10]:

$$R = 1, \quad \mathbf{Q} = (2\pi f \cdot \Delta t \cdot k_c)^2 \cdot \mathbf{I}_3 \tag{15}$$

Here, Δt is the time between successive filter updates, f is the frequency of the targeted mode. k_c is a chosen factor, typically in the range 0.2 to 0.5, where low values gives slower convergence of the filter states and a less responsive controller, and high values gives faster convergence but potentially a more erratic control signal.

The Kalman filter estimator on this form assumes knowledge of the frequency of the mode and the specific transfer function residue, and allows prediction of the amplitude and angle of the phasor based on the applied control signal. The next section describes use of this estimator in a MMAE scheme.

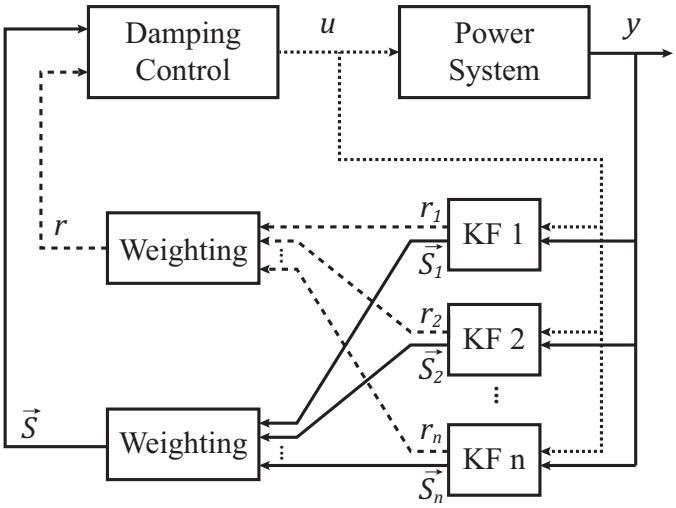

Fig. 1. A block diagram of the MMAE scheme is shown. Multiple Kalman filters (KF1, KF2,...,KFn) are running in parallel. The filters estimate the phasor based on different models. The models are determined by different assigned transfer function residues. The final phasor estimate used for generating the damping control signal is generated by weighting the individual filter state estimates. Similarly, the residue estimate, from which the phase compensation of the P-POD is determined, is generated by weighting the residue values assigned to the filters. The weighting is determined by the performance of the filters.

III. Multiple Model Adaptive Estimation: Adaptive Phasor POD

In this section, a MMAE scheme is introduced, where a number of Kalman filters are run in parallel. Each individual filter is on the form given in the previous section, but the filters differ in that they have different Control-Input Models ($\mathbf{G}_k$). The final state estimate from the filter bank is produced by weighing the state estimates of the individual filters according to a weighting function. A block diagram describing the scheme is shown in Fig. 1.

The prediction step, as given by (11), depends on the parameters associated with the residue, i.e. U and V. The filters in the filter bank are chosen such that the Control-Input Model of each filter corresponds to one specific, assigned residue. Assuming an approximate initial guess of the actual residue r_0, other variants of this residue are generated by rotation or scaling, and then one residue is assigned to each filter. In this paper, for the sake of simplicity only rotation is considered. Assuming N filters, the residues are distributed evenly around a circle with a radius determined by $|r_0|$ as follows:

$$r_i = r_0 \cdot e^{j\theta_i}, \quad \theta_i = \frac{2\pi \cdot i}{N+1}, \quad i = 1, 2, ..., N \tag{16}$$

From this, the parameters of the Control-Input Model for each filter are determined by $U_i = \mathrm{Re}\{r_i\}$ and $V_i = \mathrm{Im}\{r_i\}$. For filter i, the following model determines the prediction step:

$$\begin{bmatrix} \bar{S}_{i,k+1} \\ D_{i,k+1} \\ Q_{i,k+1} \end{bmatrix} = \begin{bmatrix} 1 & & \\ & 1 & \\ & & 1 \end{bmatrix} \begin{bmatrix} \bar{S}_{i,k} \\ D_{i,k} \\ Q_{i,k} \end{bmatrix} + \underbrace{\begin{bmatrix} 0 \\ U_i g(t) + V_i h(t) \\ -U_i h(t) + V_i g(t) \end{bmatrix}}_{\mathbf{G}_{i,k}} u_k \tag{17}$$

Due to the different residue values assigned to each filter, the performance of the filters will vary. Filters whose assigned residues are close to the actual residue will perform better, and vice versa for filters whose assigned residues are far from the actual residue. To quantify the performance of a single filter i, the residual $\varepsilon_{i,k}$ and the variance of the residual $E_{i,k}$ are introduced:

$$\varepsilon_{i,k} = Y_k - \mathbf{H}_k \mathbf{X}_{i,k} \tag{18}$$

$$E_{i,k} = \mathbf{H}_k \mathbf{P}_{i,k} \mathbf{H}_k^\intercal + R \tag{19}$$

Here, $\mathbf{P}_{i,k}$ is the Estimate Covariance Matrix. The measurement Y_k, the measurement noise variance R and the observation model $\mathbf{H}_k$ are the same for all filters in the bank. This allows the likelihood function to be calculated, which tells how likely it is that a filter is performing optimally:

$$\mathcal{L}_{i,k} = \frac{1}{\sqrt{2\pi E_{i,k}}} \exp\left[-\frac{\varepsilon_{i,k}^2}{2E_{i,k}}\right] \tag{20}$$

The weighting is determined by the likelihood functions of the filters. Initially, each filter is assigned a weight $W_{i,0} = 1/N$. Further, the filter weights are updated at each step according to the following three-step weighting scheme, inspired by the procedure in [17]:

1) Recursive update of weights:

$$W'_{i,k} = \frac{\mathcal{L}_{i,k} W_{i,k-1}}{\sum_{j=1}^{N} \mathcal{L}_{j,k} W_{j,k-1}} \tag{21}$$

2) Bounding from zero, with minimum value δ:

$$W_{i,k} = \begin{cases} W'_{i,k} & \text{if } W_{i,k} > \delta \\ \delta & \text{if } W_{i,k} \leq \delta \end{cases} \tag{22}$$

3) Normalization:

$$W_{i,k} = \frac{W_{i,k}}{\sum_{j=1}^{N} W_{j,k}} \tag{23}$$

Step 1 is the standard MMAE way of updating the weights. In Step 2, the weights are bounded from zero, which is necessary to prevent poorly performing estimators from "dying out". Step 3 normalizes the weights so the sum equals one. Finally, the MMAE state estimate is computed as the weighted sum of the state estimates of the individual filters:

$$\mathbf{X}_k = \sum_{i=1}^{N} W_{i,k} \cdot \mathbf{X}_{i,k} \tag{24}$$

In a similar fashion, the transfer function residue estimate is calculated:

$$r_k = \sum_{i=1}^{N} W_{i,k} \cdot r_{i,k} \tag{25}$$

The phase compensation β used by the P-POD is determined from the estimated residue:

$$\beta_k = 180^\circ - \arg\{r_k\} \tag{26}$$

It should be noted that if the residue estimate is close to zero (which is the case immediately after initializing the MMAE filter bank), the angle of the residue estimate is not clearly defined. Therefore, to avoid unpredictable behavior, the

phase compensation β is not updated before the magnitude of the residue estimate is above a certain threshold. In all the presented results this threshold is set to 0.2.

Tuning of the Kalman Filters

In [10], it is found that multiplying both covariance matrices R and $\mathbf{Q}$ by the same constant does not affect the power oscillation damping performance of the P-POD. However, when running multiple filters in a MMAE scheme, the weights are determined by the likelihood functions of the filters, and the likelihood functions (as defined in (20)) are not independent of the scaling of the covariance matrices. A scaling coefficient k_σ is therefore introduced in (15), which scales the covariances of all filters as follows:

$$R = k_\sigma^2, \quad \mathbf{Q} = (2\pi f \cdot \Delta t \cdot k_c k_\sigma)^2 \cdot \mathbf{I}_3 \tag{27}$$

The scaling coefficient should be chosen such that the filter weights converge fast enough (lower values of k_σ) to follow changing operating conditions, but slow enough (higher values of k_σ) to avoid erratic, unpredictable evolution of the weights. Experience indicates that choosing the scaling coefficient such that the measurement noise variance R is in the same order of magnitude as the amplitude of the targeted oscillations is a good choice. In all the presented results, this is used as a starting point for choosing the covariance scaling coefficient.

Note on changing mode frequency

During changing operating conditions, the frequency of the targeted mode should also be expected to change (not only the transfer function residue). In the above presented theory, changing mode frequency is not accounted for explicitly. A minor deviation between the assumed and the actual frequency is not expected to be problematic, as this would simply result in a slow, constant drift of the angle of the estimated phasor. The POD is thus expected to operate as intended in this case.

However, for larger frequency deviations, the performance would deteriorate. As described in [4], a frequency correction scheme can be arranged within the P-POD framework. It is expected that this scheme can be combined with the above presented theory to achieve higher robustness against larger frequency deviations (e.g. by continually updating ω in (10) and (11)). Determining the details of such an arrangement is a topic of further research.

IV. Results

In this section, the MMAE-enhanced P-POD is tested on three different systems: The Single-Machine Infinite Bus system, Kundur's Two-Area System and the IEEE 39-Bus System. All simulations are carried out entirely in Python using the simulator described in [18] (available online [19]) which was developed specifically for the purpose of testing the proposed enhancement to the P-POD. In the simulations, all generators are represented by the 6$^{\text{th}}$ order synchronous machine model described in [20] (leakage reactance, armature resistance and saturation are neglected). Simulations are carried out with a time step of 5 ms, and the Kalman filters and control signals are updated every 20 ms. Common to all three systems is that the device modulated by the P-POD is a TCSC installed on one of the lines. The TCSC is modelled as described in [12], with a steady state compensation of 10% and minimum and maximum compensation limits of 1% and 50%, respectively. Further, the parameter $k_c = 0.2$ (as suggested in [10]), the minimum bound for the weights $\delta = 0.001$, and the number of filters $N = 10$.

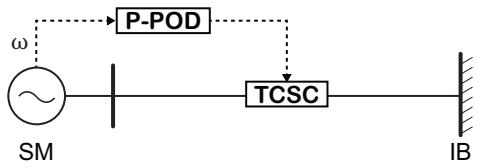

Fig. 2. The single line diagram shows the Single-Machine (SM) Infinite Bus (IB) system with a TCSC installed on the line. The P-POD measures the speed of the generator, and controls the TCSC.

A. Single-Machine Infinite Bus: Comparison with state of the art

In this section, the proposed adaptive P-POD is demonstrated and compared with an adaptive phase compensation scheme for the P-POD found in the literature: In [7] and [8], the P-POD is made adaptive by controlling the compensation angle using a Proportional Integral (PI) controller, aiming to drive the magnitude of the oscillations towards zero,

$$\beta(t) = -K_p \times |\vec{S}(t)| - K_i \times \int |\vec{S}(t)| dt \tag{28}$$

where K_p and K_i are the proportional and integral gains. However, this scheme assumes that the P-POD is actually able to eliminate the oscillations completely. Considering the situation where the phase compensation β is initially at its optimal value, it is clear that β will immediately start drifting off this optimal value once oscillations are observed again, due to the integral of the magnitude of the phasor $|\vec{S}(t)|$.

This PI control-based phase compensation scheme is compared with the proposed MMAE-based scheme. The covariance scaling coefficient $k_\sigma = 1$ for the filters in the MMAE filter bank. For the PI controller, the proportional and integral gains are $K_i = 1$ and $K_p = 1$. The control signal is amplified with gain $K = 0.2$ in both cases. The simulated system is a Single-Machine Infinite Bus system, with parameters given in [14, p. 752]. The output measurement is the rotor speed of the synchronous machine (in %pu), and the control signal modulates the reactance setpoint of a TCSC installed on the line. The system is shown in Fig. 2.

The simulated case contains three consecutive short circuits (at $t = 1$ s, $t = 15$ s and $t = 30$ s) at the terminals of the synchronous machine. Moreover, to test the capability of the two methods to properly adjust the phase compensation, an extra challenge is introduced: From the time of the second short circuit and onwards, a polarity reversal of the output from the controllers is simulated by multiplying the control signal by negative one. This means that an additional $180°$ is added to the actual residue angle. Thus, if the phase compensation

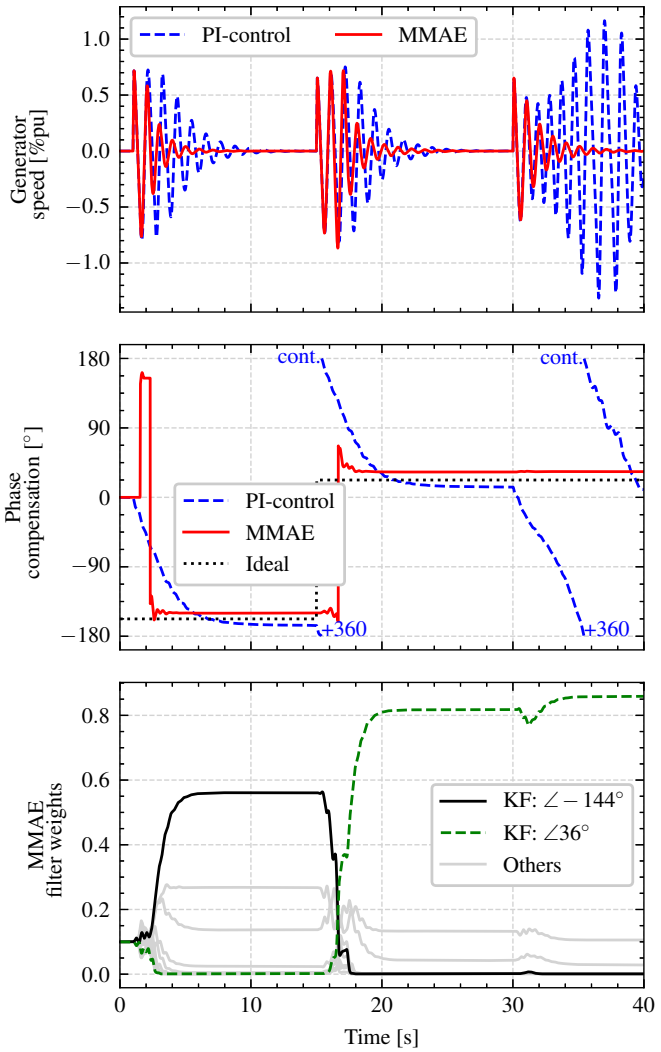

Fig. 3. Two adaptive phase compensation schemes for the P-POD are compared on the Single-Machine Infinite Bus system. During the second disturbance ($t = 15$ s), a polarity reversal of the control signal is applied, requiring the controllers to change the phase compensation by 180° to avoid forced oscillations. During the third disturbance (at $t = 30$ s), the PI control-based scheme exhibits a weakness in that the phase compensation drifts away from a suitable value, causing forced oscillations for a short period. Thus, the MMAE scheme outperforms the PI control scheme in this case.

is not adjusted at this point, the controllers will amplify rather than mitigate the oscillations.

The results from the two simulations are shown in Fig. 3. It is observed that after the first short circuit, the ideal phase compensation is approximately reached for both controllers. Similarly, after the second short circuit, the phase compensation is adjusted to cope with the polarity reversal in both cases. However, after the third short circuit it is clear that the PI-controlled phase compensation drifts away from the ideal value, as postulated, causing growing oscillations for a short period until the phase compensation again starts converging towards the ideal value. For the proposed MMAE-based scheme, the estimated phase compensation stays close to the ideal value. Thus, the MMAE-based scheme outperforms the PI control-based scheme in this case.

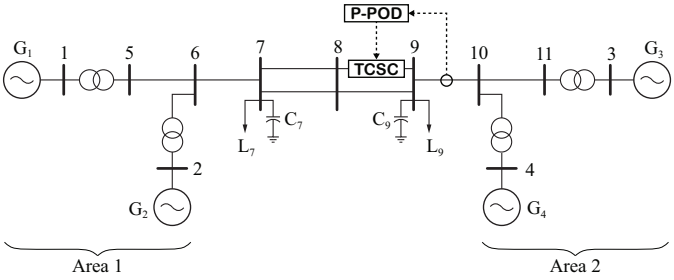

Fig. 4. The single-line diagram shows Kundur's Two-Area System. The locations where the TCSC is installed and where the measurement for the P-POD is obtained are indicated. (Source: Adapted from [14].)

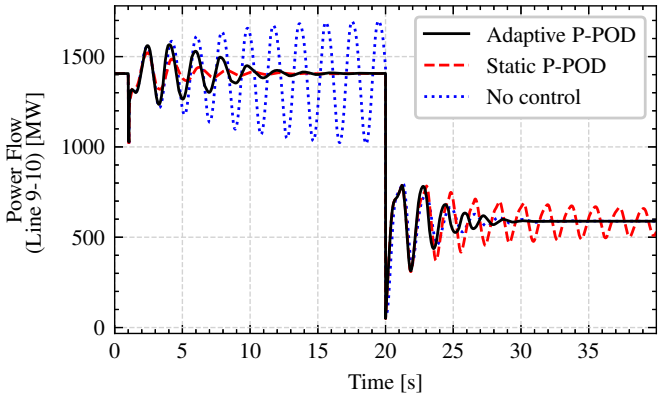

Fig. 5. The results from three simulations from Kundur's Two-Area System are shown, as indicated. At $t = 20$ s, the largest load is disconnected. Prior to the loss of load, the uncontrolled system is unstable, and the two controlled cases are stable. After the loss of load, the static P-POD is unstable; only the adaptive P-POD is stable following both disturbances. This emphasizes the need for an adaptive controller.

It is important to note that the PI-controlled phase compensation will exhibit the demonstrated weakness regardless of the tuning of the parameters K_i and K_p, since the integral of a strictly positive quantity (the magnitude of the phasor $|\vec{S}(t)|$) will always be monotonically increasing. Higher gains would cause more rapid convergence towards new operating points, but would also cause the phase compensation to drift off the ideal value faster. Similarly, lower gains would cause slower convergence towards new operating points, and also slower drift away from the ideal phase compensation.

The lower subplot in Fig. 3 shows how the weights for the MMAE scheme evolve during the simulation. Following the first disturbance, the weight of the filter corresponding to a phase compensation of $-144°$ dominates, causing a phase compensation close to this value. Following the polarity reversal, the 36° filter dominates.

B. Kundur's Two-Area System: Loss of load

In this section, the proposed controller is tested on the often used two-area system, described in [21], which consists of two areas with two generators in each area. The two areas are interconnected by long transmission lines. All the generators are equipped with AVR and governor controls, but the stabilizers are deactivated. Modal analysis reveals that the

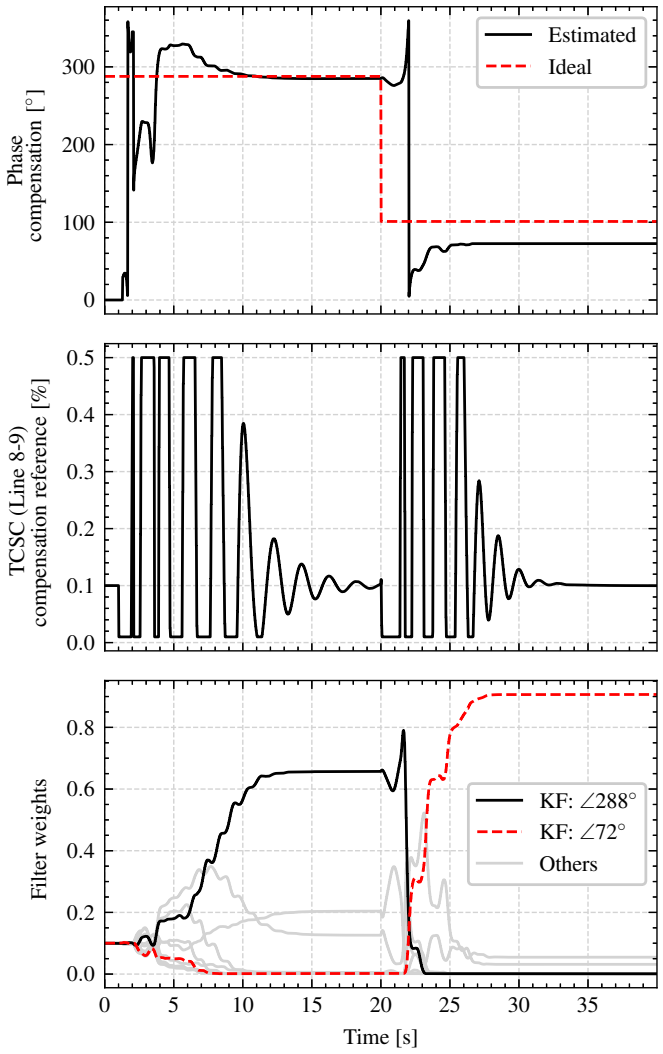

Fig. 6. From the simulation on Kundur's Two-Area System with the proposed MMAE P-POD, the phase compensation, the control signal and the evolution of the filter weights are shown. The phase compensation is shown along with the ideal value (computed from modal analysis). The control signal varies between the TCSC compensation limits of 1% and 50%. The filter weights shows that the filter corresponding to a phase compensation of 288° dominates before the loss of load, and after the loss of load the 72°-filter is the dominant.

system has an unstable inter-area mode under these conditions, with a frequency of 0.54 Hz and damping of -3%.

Similarly as in the previous case, we would like to measure the power flow in a line and modulate the reactance reference of a TCSC in order to provide damping to the unstable inter-area mode. A preliminary residue analysis reveals that measuring the power flow in the line between buses 9 and 10 and modulating a TCSC on one of the inter-ties is a good choice. For reference, this is also the combination used for a similar problem in [22]. A single line diagram is given in Fig. 4. The gain $K = 0.01$ is used for the P-POD, and the covariance scaling coefficient for the MMAE scheme is $k_\sigma = 180$. The simulated event is a short circuit with a clearing time of 50 ms, which occurs at $t = 1$ s. Further, to test the capability of the adaptive controller to adjust to changing operating conditions, a loss of the largest load in the

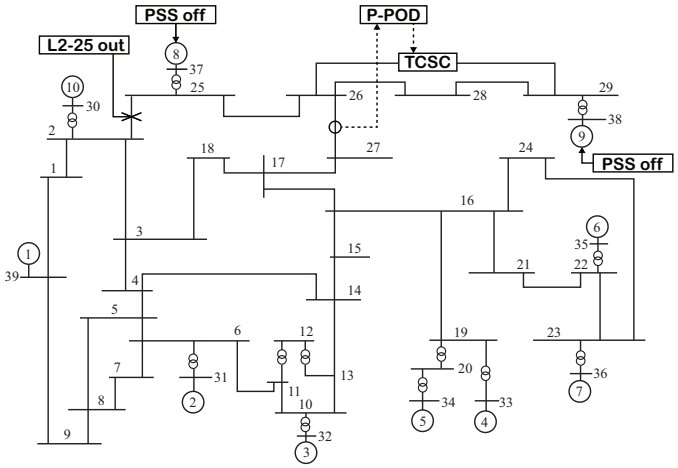

Fig. 7. The single line diagram shows the IEEE 39-Bus System, consisting of 39 buses and 10 generators. The system is stressed by deactivating two stabilizers and disconnecting a line, as indicated. (Source: Adapted from [23].)

system (1767 MW on bus 9) occurs at $t = 20$ s.

Fig. 5 shows the active power measured in the line for three different cases, first: No control action being applied, second: A static (non-adaptive) P-POD with a constant phase compensation, third: The proposed adaptive P-POD with a MMAE estimator, where the phase compensation is adjusted automatically. The results show that the system is initially unstable without supplementary damping control of the TCSC. Either of the two controls successfully stabilizes the system after the first short circuit. After the loss of load, the case with no control is stable, but the static P-POD produces forced oscillations. The adaptive P-POD stabilizes the situation both before and after the loss of load.

Fig. 6 shows in detail how the adaptive P-POD functions in this case: The first plot shows the phase compensation used by the controller, along with the ideal phase compensation (which is computed from modal analysis). The second plot shows the setpoint of the TCSC, which is modulated by the controller. The third plot shows the weights of the filters, where the dominant filters before and after the loss of load are highlighted; the 288°-filter causes a phase compensation close to this value before the loss of load, and similarly for the 72°-filter after the loss of load.

C. IEEE 39-Bus System: Varying communication latency

Finally, the proposed adaptive P-POD is tested on the IEEE 39-Bus system [23]. In this case, the aim is to test the robustness of the controller against data transmission latency. This is an important practical problem that must be addressed when working with wide area control, as the time delay between sending a PMU measurement and receiving it at the control center is not necessarily negligible.

Again, the measurement and the actuator is chosen based on preliminary residue analysis: The P-POD controls a TCSC installed on the line between buses 26 and 29, and the measurement is the active power flow in the line between buses 26 and 27. A single line diagram of the system is shown in Fig. 7. To stress the system and provoke an unstable

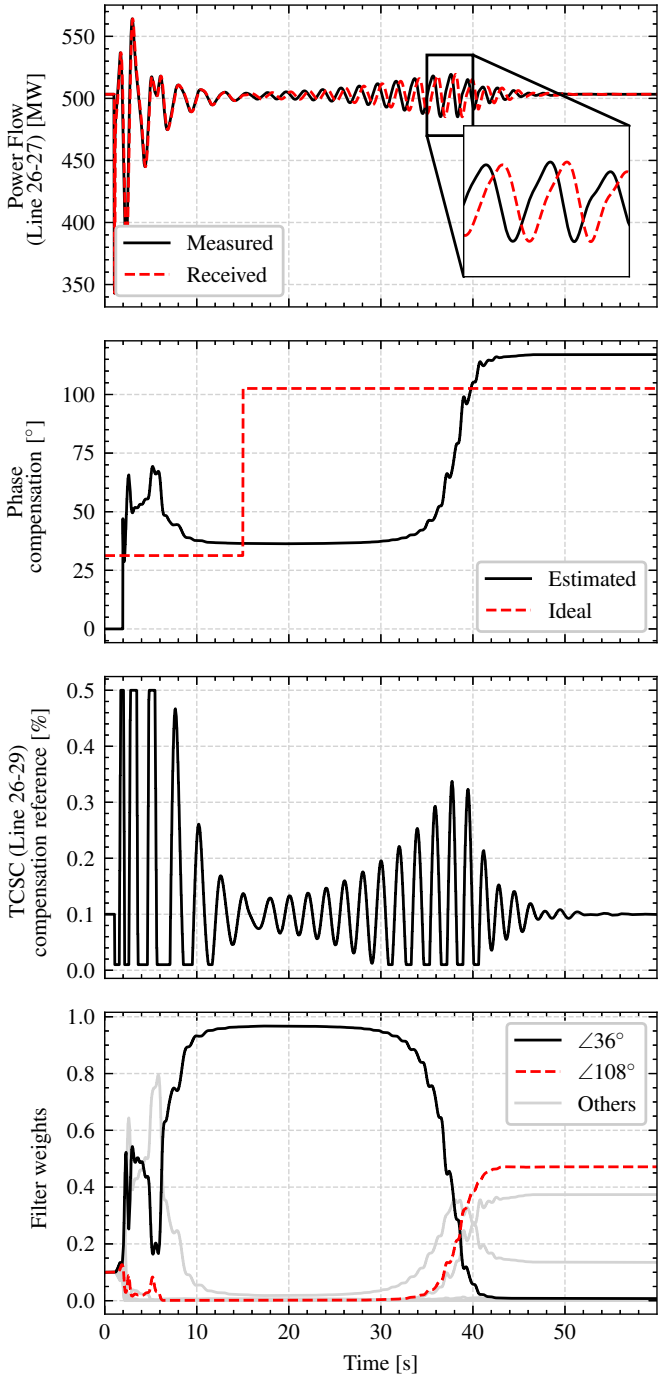

Fig. 8. Results from testing the proposed P-POD on the IEEE 39-Bus System are shown. As shown in the first plot, the received measurement at the location of the P-POD is delayed by 50 ms before $t = 15$ s, and 500 ms after $t = 15$ s. The second plot shows the phase compensation resulting from MMAE along with the ideal, latency-adjusted compensation. The third plot shows the applied control signal, and the final plot shows the evolution of the filter weights.

operating condition, the stabilizers (PSS) at generators 8 and 9 are deactivated, and the line between buses 2 and 25 is disconnected. This makes the area constituted by buses 25, 26, 28, 29 and 38 weakly connected to the rest of the system, and results in an unstable 0.44 Hz mode with zero damping. The relevant residue in this case is $26.4\angle 156°$, which gives an ideal phase compensation of $\beta = 180° - 156.6° = 23.4°$ (without latency compensation). The gain of the controller is set to $K = 0.03$, and the covariance scaling coefficient is $k_\sigma = 35$.

The simulated event is a short circuit occuring at $t = 1$ s. At the beginning of the simulation, there is a constant latency of 50 ms. At $t = 15$ s, the latency increases to 500 ms and stays constant throughout the simulation. The phase lag caused by the latency can be computed from $\omega \cdot t_{lag}$, which gives approx. $8°$ and $80°$ for the two latencies, respectively. Thus, the ideal phase compensation at the beginning of the simulation is $23.4° + 8° = 31.4°$, and after the latency increase it is $23.4° + 80° = 103°$.

The results in Fig. 8 shows that the P-POD finds a suitable phase compensation close to the ideal value after the short circuit. The latency increase causes growing oscillations for a short period, before the phase compensation is adjusted in order to cope with the phase lag caused by time delay.

V. Discussion

The proposed controller is tested on three different systems, and is capable of eliminating low damped oscillations in all cases despite drastic changes in operating conditions. In the first result, the proposed adaptive phase compensation scheme based on MMAE outperforms the PI-controlled adaptive phase compensation scheme used in [7] and [8]. The latter scheme is found to possess a weakness (i.e. drifting away from an optimal phase compensation) that the proposed scheme does not possess. In the second result, the proposed P-POD is demonstrated on a large, non-linear disturbance. The capability to adapt to changing operating conditions is a valuable trait in the future power system, where it is expected that the system will have a wider range of operating points, and the operating point will vary more rapidly. Furthermore, extreme weather is expected to become more frequent in he future, which could cause severe events like loss of large loads (as in the simulated case) to become more frequent. In the third result, the controller is tested on a significantly larger and more complex system. Robustness against latency opens up for using the P-POD in a wide-area framework, allowing remote measurements from PMUs to be used as the measurement signal for the P-POD. It should be noted, however, that sophisticated methods for alleviating the issue of latency specifically for the P-POD are developed in [7] and [8]. Combining these methods with the proposed MMAE scheme would most probably improve the result in Fig. 8.

Oscillations are successfully damped in all cases, which is the main objective. However, the ideal phase compensation is only approximately reached in some cases (e.g. in Fig. 6, the phase compensation is about 20 to 25°off the ideal value at the end of the simulation, and in Fig. 8 it is about 15 to

20°off). This can be understood by considering the fact that all filters in the MMAE filter bank are equal if the control signal is zero (as can be seen by studying (17)). Thus, if the ideal phase compensation is not reached before the oscillations are damped out, then the filter weights will stop evolving, and the final phase compensation will not be equal to the ideal value.

For each of the three cases, the controller requires tuning of the gain K (in (2)) and the covariance matrix scaling coefficient k_σ (in (27)). Also, the frequency of the low damped mode and the magnitude of the required residue are specified as parameters of the controller. Apart from this, no tuning or customization of the controller is required for each specific case.

Furthermore, the magnitude of the residue could be estimated by adding more filters to the bank. In the presented results the residues assigned to the filters differ only in rotation angle (as given by 16). More filters could be added and assigned residues with varying magnitudes, which would allow also the residue magnitude to be estimated. This would eliminate the requirement of knowledge of the residue magnitude, thus making the proposed controller more general. In practice, this would allow the proposed controller to be applied requiring only knowledge on the frequency of the targeted mode and the amplitude of oscillations. This is information that could easily be obtained from PMU measurements (e.g. using Fast Fourier Transform (FFT)). The gain, which would also have to be specified, could be increased gradually until the desired damping effect was achieved.

Replacing the algorithm in a conventional P-POD in operation today with the proposed adaptive control algorithm could allow continuous adaptation of the phase compensation during slow variations of the operating point due to load variations, potentially enhancing the performance due to a more effective phase compensation and thus a more precise damping control signal. Another application would be in a wide-area emergency damping control scheme, where the P-POD was activated once oscillations with an amplitude surpassing a specific, predefined threshold was observed. The mode frequency could be obtained quickly (within seconds) using e.g. FFT, the measurement with the highest observability of the low damped mode would be selected as the input to the controller, and a device expected to have a high controllability of the mode would be selected to carry out the damping control action (e.g. a TCSC installed on an inter-tie with high observability of the targeted mode). The phase compensation would be adjusted automatically by the MMAE scheme, eventually resulting in mitigation of the oscillations.

For the sake of simplicity the presented theory and results consider systems with only a single low damped mode. However, in large transmission systems, multiple low damped modes might be excited at the same time. Modifications to the P-POD estimation algorithm to accommodate multiple low damped modes are described in e.g. [5]. A topic of further research is to introduce similar modifications to the phasor estimation algorithm proposed in this paper. Other adaptive functionality developed within the P-POD framework, like frequency correction, latency compensation, and adaptive forgetting factor could also be combined with the proposed MMAE-based adaptive phase compensation scheme.

In 1965, when the MMAE scheme was invented, it was considered impractical for online implementation [16] due to the computational burden of running a high number of Kalman filters in parallel. However, given advances in computer technology since then, this no longer remains an issue. For the presented MMAE-based adaptive P-POD, this has been confirmed by testing all the presented systems in simulations which are synchronized to wall-clock time. By using the multiprocessing-module in Python, the simulation is run in one process, and the MMAE-based controller in another process. Testing indicates that there is no issue with operating a MMAE filter bank of 10 filters online, running on an average laptop. If a higher number of filters is required, the computational burden could easily be reduced by parallelization of the filter updates.

VI. Conclusion

In this paper, a novel adaptive Phasor Power Oscillation Damper has been developed and tested. Adaptive phase compensation is achieved by introducing a Multiple Model Adaptive Estimator, which results in a controller that requires very little tuning or customization before application to a new system. The proposed scheme outperforms a comparable scheme found in the literature under the tested conditions. It is also found that the controller performs satisfactorily during changing operating conditions caused by a large disturbance, and is capable of eliminating phase lag caused by latency.

References

[1] D. N. Kosterev, C. W. Taylor, and W. Fellow, "Model Validation for the August 10, 1996 WSCC System Outage," *IEEE Transactions on Power Systems*, vol. 14, no. 3, pp. 967–979, 1999.

[2] ENTSO-E SubGroup System Protection and Dynamics, "Analysis of CE Inter-Area Oscillations of 1st December 2016," Tech. Rep. December, 2017.

[3] ——, "Oscillation Event 03.12.2017," Tech. Rep. March, 2018.

[4] L. Ängquist and C. Gama, "Damping algorithm based on phasor estimation," in *IEEE Power Engineering Society Winter Meeting*, vol. 3, 2001, pp. 1160–1165.

[5] N. R. Chaudhuri and B. Chaudhuri, "Damping and relative mode-shape estimation in near real-time through phasor approach," *IEEE Transactions on Power Systems*, vol. 26, no. 1, pp. 364–373, 2011.

[6] N. R. Chaudhuri, S. Ray, R. Majumder, and B. Chaudhuri, "A case study on challenges for robust wide-area phasor POD," in *IEEE Power Engineering Society Winter Meeting*, 2009.

[7] ——, "A new approach to continuous latency compensation with adaptive phasor power oscillation damping controller (POD)," *IEEE Transactions on Power Systems*, vol. 25, no. 2, pp. 939–946, 2010.

[8] S. S. Yu, T. K. Chau, T. Fernando, and H. H. C. Iu, "An Enhanced Adaptive Phasor Power Oscillation Damping Approach with Latency Compensation for Modern Power Systems," *IEEE Transactions on Power Systems*, vol. 33, no. 4, pp. 4285–4296, 2018.

[9] M. Beza and M. Bongiorno, "A Modified RLS Algorithm for Online Estimation of Low-Frequency Oscillations in Power Systems," *IEEE Transactions on Power Systems*, vol. 31, no. 3, pp. 1703–1714, 2016.

[10] H. Haugdal, K. Uhlen, and H. Jóhannsson, "Achieving increased Phasor POD performance by introducing a Control-Input Model," *arXiv:2111.00968*, 2021.

[11] I. Zenelis, X. Wang, and I. Kamwa, "Online PMU-Based Wide-Area Damping Control for Multiple Inter-Area Modes," *IEEE Transactions on Smart Grid*, vol. 11, no. 6, pp. 5451–5461, 2020.

[12] B. Chaudhuri, R. Majumder, and B. C. Pal, "Application of multiple-model adaptive control strategy for robust damping of interarea oscillations in power system," *IEEE Transactions on Control Systems Technology*, vol. 12, no. 5, pp. 727–736, 2004.

[13] V. Pradhan, A. M. Kulkarni, and S. A. Khaparde, "A Model-Free Approach for Emergency Damping Control Using Wide Area Measurements," *IEEE Transactions on Power Systems*, vol. 33, no. 5, pp. 4902–4912, 2018.
[14] P. Kundur, *Power System Stability and Control*. New York: McGraw-Hill, 1994.
[15] X. Yang and A. Fellachi, "Stabilization of inter area oscillation modes through excitation systems," *IEEE Transactions on Power Systems*, vol. 9, no. 1, pp. 494–502, 1994.
[16] R. G. Brown and P. Y. C. Hwang, *Introduction to random signals and applied Kalman filtering*, 4th ed. Hoboken, NJ: Wiley, 2012.
[17] J. F. Martin, A. M. Schneider, and N. T. Smith, "Multiple-Model Adaptive Control of Blood Pressure Using Sodium Nitroprusside," *IEEE Transactions on Biomedical Engineering*, vol. BME-34, no. 8, pp. 603–611, 1987.
[18] H. Haugdal, K. Uhlen, and H. Johannsson, "An Open Source Power System Simulator in Python for Efficient Prototyping of WAMPAC Applications," in *2021 IEEE Madrid PowerTech*. IEEE, 2021, pp. 1–6. [Online]. Available: https://ieeexplore.ieee.org/document/9494770/
[19] H. Haugdal, "DynPSSimPy," *Zenodo*, 2020. [Online]. Available: http://doi.org/10.5281/zenodo.4290126
[20] J. Machowski, J. Bumby, and J. Bialek, *Power system dynamics: Stability and control*, 2nd ed. Wiley, 2008.
[21] M. Klein, G. J. Rogers, and P. Kundur, "A fundamental study of inter-area oscillations in power systems," *IEEE Transactions on Power Systems*, vol. 6, no. 3, pp. 914–921, 1991.
[22] B. Pal and B. Chaudhuri, *Robust Control in Power Systems*, ser. Power Electronics and Power Systems. Boston: Springer US, 2005.
[23] M. A. Pai, *Energy Function Analysis for Power System Stability*. Boston, MA: Springer US, 1989.

Hallvar Haugdal received the M.Sc. degree in electrical power engineering from the Norwegian University of Science and Technology (NTNU) in 2016. He is currently pursuing his Ph.D. on Wide Area Monitoring and Control. Current research interests include power system dynamics and simulation, electromechanical oscillations and electric machines.

Kjetil Obstfelder Uhlen received the master's and Ph.D. degrees in control engineering in 1986 and 1994 respectively. He is a Professor of power systems with the Norwegian University of Science and Technology (NTNU), Trondheim, and a Special Adviser at STATNETT (the Norwegian TSO). His main areas of work include research and education within control and operation of power systems, grid integration of renewable energy, and power system dynamics.

Hjörtur Jóhannsson (M'11) received the M.Sc. and Ph.D. degrees in electrical engineering from the Technical University of Denmark, Kongens Lyngby, Denmark, in 2007 and 2011, respectively, where he is currently a Senior Scientific Consultant with the Center of Electric Power and Energy, Department of Electrical Engineering. His research interests include the development of methods for secure and stable operation of power systems with a high share of RES-based production, with special focus on real-time approaches.